Novel Near-Infrared Squaraine Sensitizers for Stable and Efficient Dye-Sensitized Solar Cells

*Chuanjiang Qin, Youhei Numata, Shufang Zhang, Xudong Yang, Ashraful Islam, Kun Zhang, Han Chen, and Liyuan Han**

A new molecular design strategy for tuning the energy levels of *cis*-configured squaraine sensitizers for dye-sensitized solar cells is described. The Hammett substituent constant and the π-conjugation length are used as quantitative indicators to modify the central squarate moiety of the sensitizer dyes; specifically, novel near-infrared squaraine dyes HSQ3 and HSQ4 are synthesized by incorporation of an electron-withdrawing and π-extending ethyl cyanoacetate unit on the central squarate moiety. The solution absorption maximum of HSQ4 occurs at 703 nm, and the energy levels of the lowest unoccupied molecular orbital and the highest occupied molecular orbital are in the ideal range for energetically efficient electron injection and regeneration of the oxidized dye. A solar cell sensitized with HSQ4 exhibits a broad incident photon-to-current conversion efficiency spectrum, extending into the near-infrared region with a maximum value of 80% at 720 nm, which is is the highest value reported for a squaraine dye–based dye-sensitized solar cell. The HSQ4-sensitized solar cell also exhibits excellent durability during light soaking, owing to the double anchors attaching the dye to the TiO_2 surface and to the long alkyl chains extending outward from the surface.

1. Introduction

Dye-sensitized solar cells (DSCs) are receiving increasing attention as a renewable energy source owing to their potential use in low-production-cost, large-area, flexible, colorful, and lightweight devices.[1] A key strategy for the development of practical DSCs is the replacement of ruthenium-based sensitizer dyes with organic dyes that have higher absorption extinction coefficients and lower materials costs and are amenable to molecular tailoring.[2] Among the various types of organic sensitizers, near-infrared (NIR) sensitizers, such as porphyrins,[3] phthalocyanines,[4] cyanines,[5] and squaraines,[6] are the most appealing because they absorb strongly in the red and NIR regions. Such NIR dyes have been employed as co-sensitizers to improve the photovoltaic properties of DSCs.[7] In addition, NIR dyes exhibit low or no absorption intensity in the visible region and can therefore be used in tandem DSCs and transparent and/or colorless photovoltaic devices.[8]

Squaraine dyes have been widely used in DSCs, as well as in solution-processable bulk heterojunction and vacuum-deposited solar cells.[9] Since 2007, when sensitization with squaraine dye SQ1 was reported to greatly increase the energy conversion efficiency (η of DSCs (**Scheme 1**),[10] many researchers have attempted to prepare even better squaraine dyes by linearly extending the π-conjugation of the backbone.[11] For example, Kuster et al. synthesized BSQ01, an unsymmetrical squaraine dimer with a linear connector, which extended the onset wavelength of the incident photon-to-current conversion efficiency (IPCE) response to around 780 nm.[12] However, the maximum IPCE achieved with this dye is only 17% at 740 nm with an η of 1.3% because the thermodynamic driving force is not sufficient for efficient electron injection into the conduction band of TiO_2 and because the dye aggregates on the TiO_2 surface. The IPCE responses of various other modified squaraine dyes in the NIR region are also low (less than 50% at 700 nm) for the same reasons.[13] Therefore, the development of a new strategy for tuning the dye energy levels by simple structural modification is necessary for achieving a red-shifted IPCE response with a high η.

Recently, we red-shifted the IPCE response of squaraine dyes by introducing a strongly electron-withdrawing dicyanomethylene group into the central squarate moiety.[14] The resulting new squaraine dye, HSQ1, adopts a *cis* configuration, and the absorption maximum is remarkably red-shifted (by 39 nm) compared with that of SQ1. The maximum IPCE we have achieved with an HSQ1-sensitized DSC is 71% at 700 nm. However, the lowest unoccupied molecular orbital (LUMO) and the highest occupied molecular orbital (HOMO) of HSQ1 are still not ideal for energetically efficient electron injection and regeneration of the oxidized dye, respectively.[15]

For fine-tuning the energy levels and preparing more-efficient substituted squaraine dyes, the development of a systematic strategy for molecular design is important. We focused on the Hammett substituent constant and π-conjugation length as

Dr. C. Qin, Dr. Y. Numata, Dr. S. Zhang, Dr. X. Yang, Dr. A. Islam, K. Zhang, Dr. L. Han
Photovoltaic Materials Unit
National Institute for Materials Science
Sengen 1–2–1, Tsukuba, Ibaraki, 305–0047, Japan
E-mail: HAN.Liyuan@nims.go.jp
Dr. H. Chen, Dr. L. Han
State Key Laboratory of Metal Matrix Composites
Shanghai Jiao Tong University
800 Dong Chuan Road, Shanghai, 200240, China

DOI: 10.1002/adfm.201303769

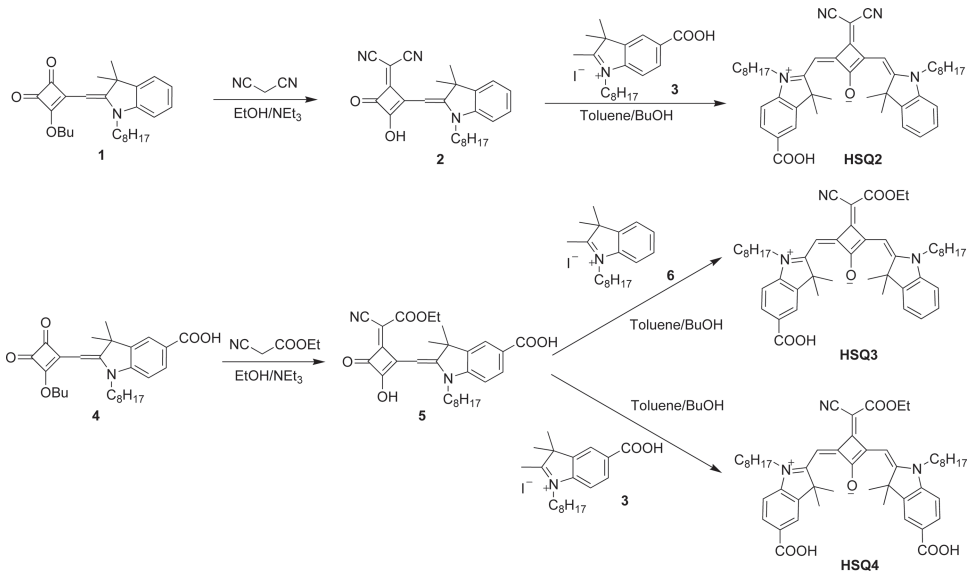

Scheme 1. Syntheses of HSQ2, HSQ3, and HSQ4.

quantitative indicators for choosing appropriate substituents, and we prepared squaraines HSQ2 (a homologue of HSQ1 containing two octyl chains), HSQ3, and HSQ4 (**Figure 1**). The Hammett substituent constants of the –COOEt and –CN groups (σ_{COOEt} and σ_{CN}, respectively) are 0.297 and 0.579,[16] indicating that –COOEt is less electron withdrawing than –CN; therefore, we expected that the former might raise the energy levels of both the HOMO and the LUMO. These two substituents have similar conjugation lengths, so we expected that *cis*-configured HSQ3 would have the same the narrow band gap as

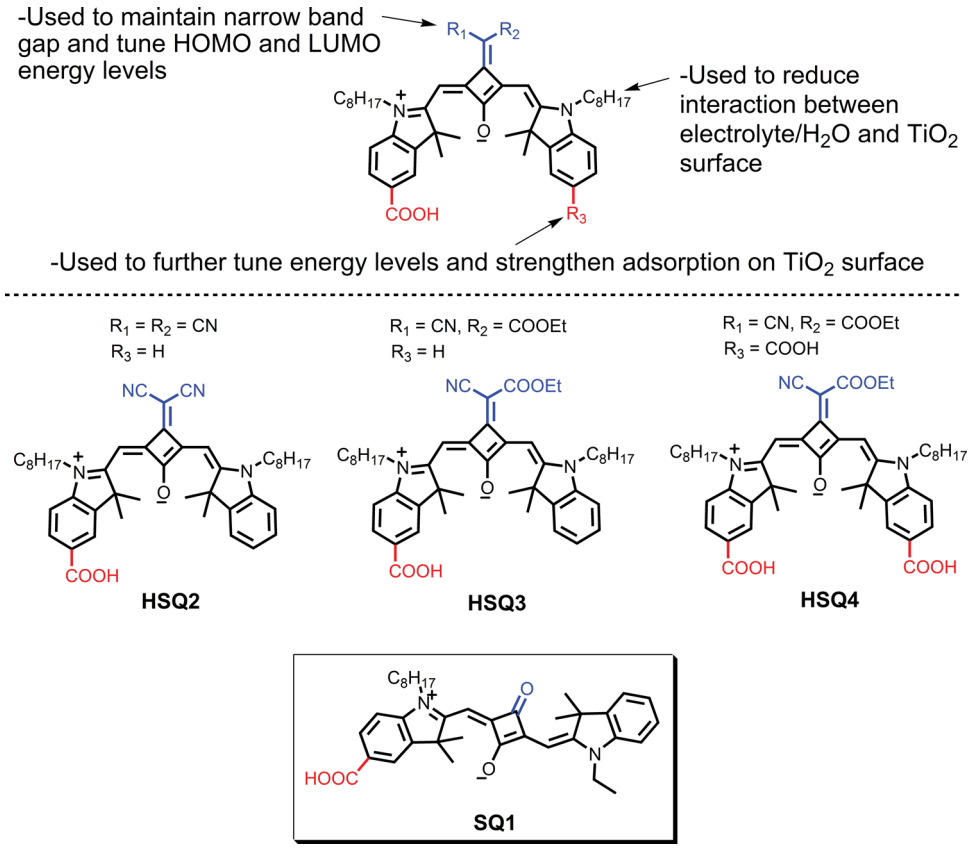

Figure 1. Molecular design elements and structures of squaraine sensitizers HSQ2, HSQ3, and HSQ4, along with the structure of SQ1.

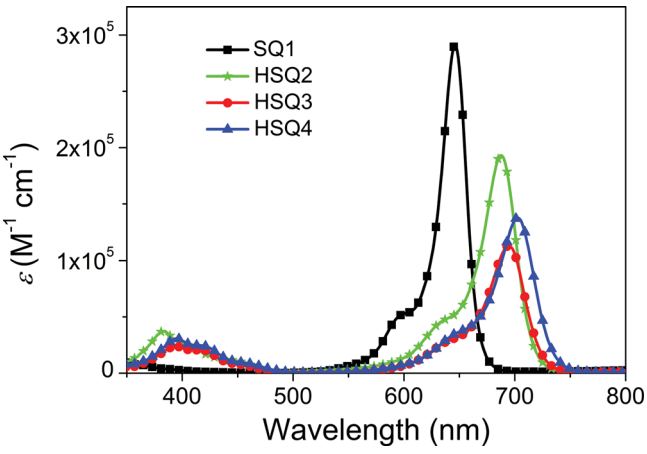

Figure 2. Absorption spectra of squaraine dyes in DMF.

Table 1. Photophysical and electrochemical data for SQ1, HSQ2, HSQ3, and HSQ4.

Dye	λ_{max} in DMF [nm] (ε)[a)]	λ_{max} on TiO_2 [nm][b)]	E_{0-0} [eV][c)]	E_{ox} [V][d)]	E_{ox}* [V][e)]
SQ1	647 (2.92)	641	1.85	0.83	–1.02
HSQ2	688 (1.93)	690	1.77	0.92	–0.85
HSQ3	695 (1.13)	703	1.75	0.70	–1.05
HSQ4	703 (1.37)	711	1.74	0.74	–1.00

[a)]Absorption peaks and molar extinction coefficients (ε) were measured in DMF (2×10^{-6} M); the unit for ε is 10^5 M^{-1} cm^{-1}; [b)]The TiO_2 film thickness was 4 μm; [c)]Optical energy gaps (E_{0-0}) were calculated from the intersection of normalized absorption and photoluminescent spectra; [d)]First ground-state oxidation potentials (E_{ox}) were measured in CH_2Cl_2 (vs NHE); [e)]First-excited-state oxidation potentials (E_{ox}*) were calculated from $E_{ox}^* = E_{ox}^0 - E_{0-0}$ (vs NHE).

HSQ2. To further narrow the band gap, we attached a second –COOH group to the indolinium moiety to afford HSQ4.

By means of this rational molecular design strategy, we were able to bathochromically shift the solution absorption maximum from 688 nm for HSQ2 to 703 nm for HSQ4. The IPCE spectrum of HSQ4 exhibited a high, broad plateau extending into the NIR region, with a maximum value of 80% at 720 nm. Of all the squaraine dyes reported to date, HSQ4 has the highest IPCE response in the NIR region. Using HSQ4, we constructed a DSC that showed a conversion efficiency of 5.66%. Furthermore, the HSQ4-sensitized solar cell exhibited excellent durability on light soaking for two reasons: 1) the two anchoring groups increased the adsorption stability of the sensitizer on the TiO_2 surface and 2) the long alkyl chains extending outward from the *cis*-configured dye formed a hydrophobic layer above the dye monolayer on the TiO_2 surface.

2. Results and Discussion

2.1. Synthesis

The syntheses of HSQ2, HSQ3, and HSQ4 are shown in Scheme 1. The synthesis of HSQ2 was similar to our previously published synthesis of HSQ1.[14] Condensation of semisquaraine derivative **4** and ethyl cyanoacetate yielded key intermediate **5** for the syntheses of HSQ3 and HSQ4. Although ethyl cyanoacetate is a weaker electron-withdrawing group than a dicyano group, **5** still displayed high reactivity toward nucleophilic methylene bases, and HSQ3 and HSQ4 were obtained in good yields from the reactions of **5** with **3** and **6**, respectively, in refluxing 1:1 toluene/*n*-butanol. The dye products were fully characterized by ^1H and ^{13}C NMR, elemental analysis, and HRMS. Both dyes dissolved readily in common organic solvents, such as chloroform, DMF, and methanol.

2.2. Absorption Spectroscopy

As shown in **Figure 2** and **Table 1**, DMF solutions of HSQ2, HSQ3, and HSQ4 showed two main absorption bands, one in the long-wavelength region and another in the blue region, which were assigned to the S_1 and S_2 transitions, respectively.[14,17] The λ_{max} of the S_1 transition of HSQ3 (695 nm) was red-shifted by 7 nm relative to that of HSQ2. This bathochromic shift was attributed to introduction of the ethyl cyanoacetate group, which raised the HOMO energy level to a greater degree than it raised the LUMO energy level relative to those of the dicyano dye (vide infra). Furthermore, DFT calculations have indicated that the ethyl cyanoacetate unit can be expected to maintain its electron-withdrawing strength in the ground state and to possess π-donor character in the excited state of the dye.[18] This expectation was confirmed and is discussed below in the electrochemical characterization section. The introduction of a second –COOH group on the indolinium moiety of HSQ4 led to a further 8-nm bathochromic shift; in addition, the molar extinction coefficient of HSQ4 (1.37×10^5 M^{-1} cm^{-1}) was higher than that of HSQ3 (1.13×10^5 M^{-1} cm^{-1}) owing to the weak electron-withdrawing ability of the –COOH group and the symmetric structure of the former molecule. Thus, by means of our rational molecular design strategy, we were able to achieve a total bathochromic shift of 56 nm for HSQ4 relative to SQ1.

The trend in the absorption spectra of the four squaraine dyes adsorbed on TiO_2 films was similar to the trend for the solution spectra; a slight bathochromic shift due to interaction between the dye molecules and TiO_2 was observed (**Figure 3**). Note that the absorption peak of HSQ4 was red-shifted by 21 nm compared to that of HSQ2, and reached 711 nm with an absorption onset at 800 nm. Moreover, the absorptions of HSQ3 and HSQ4 below 500 nm were stronger than the absorption of SQ1; this change will facilitate light capture and improve IPCE response in this high-energy region.

2.3. FTIR and ATR-FTIR Spectra

Comparison of the Fourier transform infrared (FTIR) spectrum of HSQ4 on a KBr pellet and the attenuated total reflectance FTIR spectrum of the dye adsorbed on TiO_2 revealed that the band at 1679 cm^{-1} (C = O stretching of the aromatic carboxylic acid) in the former was not present in the latter (Figure S1, Supporting Information). This result indicates that HSQ4 was anchored to the TiO_2 surface via both –COOH groups. The CN

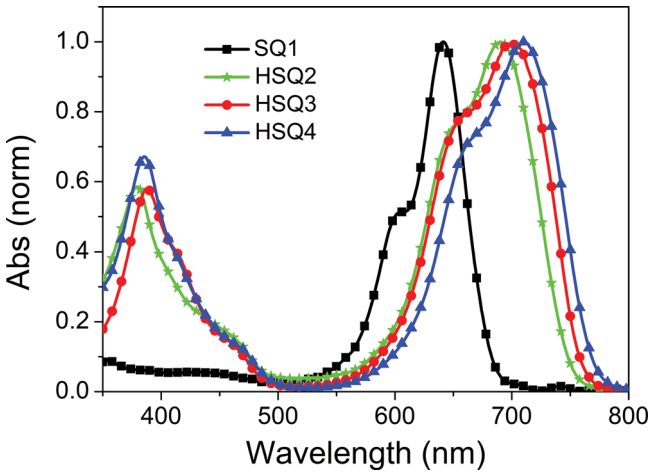

Figure 3. Normalized absorption spectra of squaraine dyes on TiO_2 (film thickness: 4 μm).

stretching band at 2190 cm^{-1} and the C = O stretching band of the –COOEt group at 1715 cm^{-1} in the spectrum of the adsorbed dye were similar to the corresponding bands in the FTIR spectrum, which means that the ethyl cyanoacetate group was free and far from the TiO_2 surface. Taken together, these results suggest that the octyl groups extended outward from the TiO_2 surface. As we proposed above, all these characteristics can be expected to improve final cell stability.

2.4. Electrochemical Properties

The redox potentials of the four squaraine dyes were measured by cyclic voltammetry (**Figure 4** and Table 1). HSQ2, HSQ3, and HSQ4 exhibited first oxidation potentials (E_{ox}) at 0.92, 0.70, and 0.75 V (vs NHE, Figure S2, Supporting Information), respectively. As described above, –CN is more electron withdrawing than –COOEt, which is consistent with the observed change in the oxidation potential. The oxidation potentials were low enough for efficient regeneration of the oxidized dyes via electron donation from iodide (≈0.4 V vs NHE). Moreover, the lower oxidation potentials of HSQ3 and HSQ4 relative to that of HSQ2 should reduce the energy loss (ΔG_2, Figure 4) associated with regeneration. The optical energy gaps ($E_{0\text{-}0}$) of HSQ2, HSQ3, and HSQ4 were 1.77, 1.75, and 1.74 eV, which were calculated from normalized absorption and emission spectra (Figure S3, Supporting Information). Therefore, the excited-state oxidation potentials (E_{ox}*) of HSQ2, HSQ3, and HSQ4 were –0.85, –1.05, and –1.00 V (vs NHE), respectively. The more negative E_{ox}* values of HSQ3 and HSQ4 compared to the value of HSQ2 may result in a larger driving force for electron injection from the excited state of the sensitizer to the TiO_2 conduction band (ΔG_1, Figure 4).

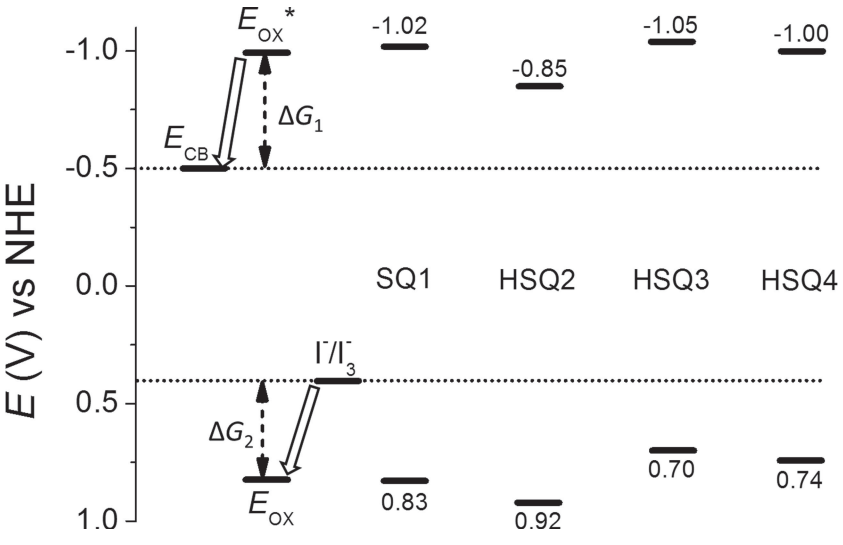

Figure 4. Electrochemical data and energy level diagrams of TiO_2, I^-/I_3^-, and the squaraine dyes.

2.5. Computational Analysis of Structure and Electron Distribution

To improve our understanding of the effects of the substituents on the molecular geometry and electronic structure of the dyes, we used DFT and time-dependent DFT for structural optimization and calculation of the frontier molecular orbital distributions (Figure S4, Supporting Information). Like the frontier molecular orbitals of HSQ2, the HOMOs of HSQ3 and HSQ4 are localized mainly on the squarate core and extend to the ethyl cyanoacetate moiety. The LUMOs are delocalized along the backbone of the molecules, and the LUMO+1s are localized on the central core and the carboxylate-substituted indolinium moieties. In particular, the LUMO+1 of HSQ4 extends to both sides of the two anchoring groups, which will favor highly efficient electron injection. The electron density distributions of HSQ3 and HSQ4 are ideally suited to facilitate efficient injection of electrons from the photoexcited dye molecule into the TiO_2 conduction band.[14]

The trends in the absorption spectra and relative oscillator strengths (*f*) of HSQ3 and HSQ4 calculated by time-dependent DFT were the same as the trends observed in the corresponding experimental results (Figure S5 and Table S1, Supporting Information). The lowest-lying electronic transition of HSQ4 (mainly excitation from the HOMO to the LUMO) was red-shifted by approximately 18 nm compared with that of HSQ2. The introduction of the ethyl cyanoacetate group and the additional –COOH group simultaneously raised the HOMO and LUMO energy levels, maintaining the narrow band gap, and led to an additional higher-energy electronic transition in the blue region (HOMO to LUMO+1 transition).

2.6. Photovoltaic Performance of DSCs

The maximum of the IPCE spectrum of a SQ1-based DSC was 80% at 650 nm (**Figure 5**). The IPCE spectrum of the HSQ2

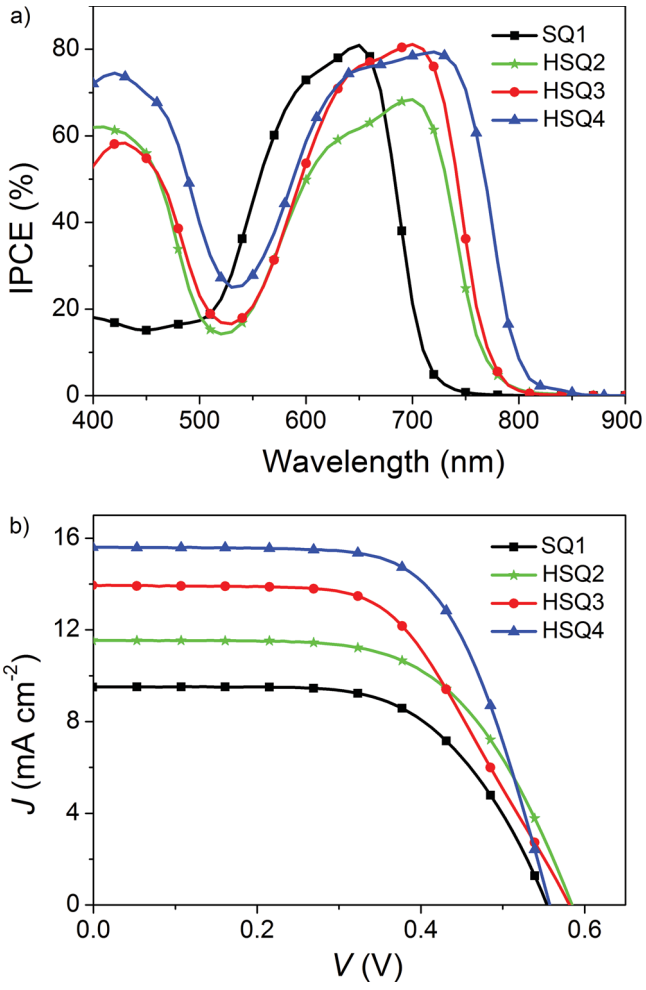

Figure 5. a) IPCE spectra and b) *I–V* curves for DSCs based on the four squaraine dyes. The electrolyte was composed of 0.6 M dimethylpropylimidazolium iodide, 0.05 M I_2, and 0.1 M LiI in acetonitrile.

cell was red-shifted by 50 nm compared with that of the SQ1 cell. However, the maximum IPCE decreased to 68% at 700 nm; we attributed this decrease to the reduction potential of HSQ2 being too low (–0.85 V, Figure 4) for efficient electron injection. A similar phenomenon has been reported in the literature;[19] a large red shift in the absorption spectrum often decreases the LUMO energy level to below the minimal acceptable level, and therefore, the IPCE response decreases.

As we expected, under the same conditions, the relatively low E_{ox}* values of HSQ3 and HSQ4 led to a significant improvement in IPCE response, owing to the larger ΔG_1. The IPCE maxima of the HSQ3 and HSQ4 cells were 81% at 700 nm and 80% at 720 nm, respectively, which are comparable to the maximum of the SQ1 cell and remarkably elevated compared with that of the HSQ2 cell in the region from 400 to 800 nm. In particular, the IPCE response of the HSQ4 cell remained high (>70%) in the region from 620 to 750 nm, and the onset wavelength of the IPCE response reached 805 nm. To the best of our knowledge, the IPCE response of the HSQ4 cell (80% at 720 nm) is the highest value reported for a squaraine dye–based DSC. Our results suggest that the electron injection efficiency

Table 2. Photovoltaic data obtained under AM 1.5G irradiation.

Dye	J_{SC} [mA cm^{-2}]	V_{OC} [mV]	FF	η [%]	IPCE [%] (at nm)
SQ1	9.51	554	0.62	3.27	81 (650)
HSQ2	11.55	584	0.61	4.11	68 (700)
HSQ3	13.95	581	0.57	4.60	81 (700)
HSQ4	15.61	558	0.65	5.66	80 (720)

in the NIR region could be improved by introduction of ethyl cyanoacetate to finely tune the energy levels.

The overall conversion efficiency (η) of the SQ1 cell was 3.27% with a short-circuit photocurrent density (J_{SC}) of 9.51 mA cm^{-2}, an open-circuit voltage (V_{OC}) of 554 mV, and a fill factor (FF) of 0.62 (**Table 2**). The η value of the HSQ2 cell (4.11%) was higher than that of the SQ1 cell owing to the large increase in the photocurrent, which originated from the broad IPCE response of HSQ2. The superior performances of the HSQ3 and HSQ4 cells were manifested in the increases in J_{SC} (13.95 mA cm^{-2} and 15.61 mA cm^{-2}) compared to the J_{SC} of HSQ2 (11.55 mA cm^{-2}), which was in good accord with the improved IPCE response over all regions. The V_{OC} of the HSQ4 cell (558 mV) was slightly lower than that of the HSQ3 cell (581 mV). This difference may have been the result of substantial charge recombination in the HSQ4 cell, because the HOMO of HSQ4 was closer to the TiO_2 surface which is ascribed to its adsorption status on the surface via two anchors. Electrochemical impedance spectroscopy data (Figure S6, Supporting Information) indicated that the HSQ4 cell showed smaller resistance to electron recombination than the HSQ3 cell, which further explained the lower V_{OC} of the former. Finally, the η value of 5.66% for the HSQ4 cell was obtained as a result of the superior J_{SC} and FF. It is noteworthy that HSQ4 is the first NIR squaraine sensitizer with a high IPCE response (80%) at a wavelength longer than 700 nm and a high conversion efficiency.

2.7. Stability of DSCs

Because most DSCs based on squaraine dyes demonstrate low durability, we evaluated the durability of DSCs sensitized with each of the three squaraine sensitizers under visible light–soaking conditions at room temperature with a binary ionic liquid–based electrolyte.

The three DSCs demonstrated completely different behaviors after long-duration light soaking (**Figure 6**). The benchmark SQ1 cell showed the worst durability, which we ascribed to desorption and/or decomposition of the sensitizer because the color of the sensitized TiO_2 film changed from deep blue to gray after 1000 h of light soaking. The HSQ3 cell was more stable, owing to the octyl chains extending outward from the TiO_2 surface. The long hydroph-obic alkyl chains formed a compact hydrophobic layer above the dye monolayer on the TiO_2 surface and prevented the contact between the surface and trace H_2O in the electrolyte that would have led to desorption of dye molecules from the surface. The HSQ4 cell exhibited excellent durability. After 1000 h of light soaking, η remained

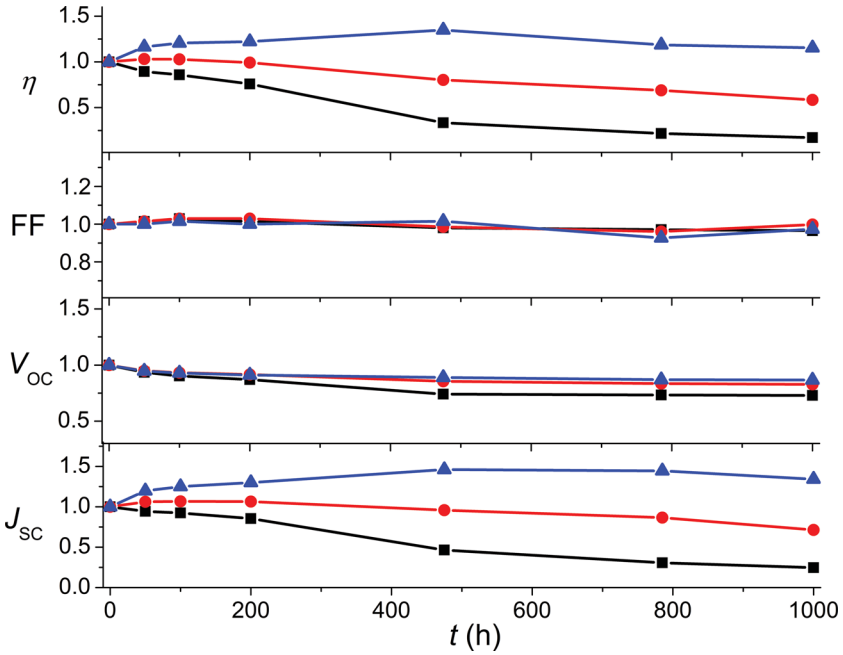

Figure 6. Evolution of normalized DSC parameters with SQ1 (squares), HSQ3 (circles), and HSQ4 (triangles) during light soaking (AM 1.5G). A 420-nm cut-off filter was applied during illumination. Ionic-liquid electrolyte: 0.15 M I_2, 0.1 M GuSCN, 0.5 M MBI, and 1 M PMII in MPN.

at its original level, and the color of the film had not changed. We ascribed the excellent long-term stability of the HSQ4 cell to the double anchors suppressing desorption of dye molecules and to the long alkyl chains.

3. Conclusions

Two new *cis*-configured squaraine dyes with an ethyl cyanoacetate unit on the central squarate moiety were synthesized. By maintaining the conjugation length and adjusting the electron-withdrawing strength by choosing the ethyl cyanoacetate, which has a small Hammett constant, we obtained a new squaraine dye, HSQ3, which showed a bathochromic shift of the S_1 transition band in comparison to that of dicyano-substituted dye HSQ2. At the same time, we tuned the HOMO and LUMO energy levels to positions more ideal for efficient electron injection and dye regeneration. The absorption peak of HSQ4 was further red-shifted to 703 nm, owing to the presence of a second –COOH group on the indolinium moiety. The dyes prepared on the basis of this rational molecular design strategy showed better performance in DSCs than the reference dyes (SQ1 and HSQ2) under the same conditions. In particular, a DSC based on HSQ4 showed a high IPCE in both the blue and NIR regions and achieved a maximum IPCE of 80% at 720 nm. Moreover, the HSQ4-sensitized solar cell demonstrated an excellent durability, which we ascribed to the double anchors and suppression of charge recombination by the alkyl groups extending outward from the TiO_2 surface. HSQ4, with its high absorption coefficient in the NIR region, represents an important breakthrough in the design of squaraine dyes for DSC applications. On the basis of these results, we are working on the further development of more-efficient squaraine dyes, as well as on co-sensitization.

4. Experimental Section

Synthesis: All chemicals and reagents were used as received from suppliers without further purification. 3-Butoxy-4-[(1-octyl-3,3-dimethyl-1,3-dihydro-2*H*-indol-2-ylidene)methyl]-3-cyclobutene-1,2-dione (1), 3-hydroxy-2-[(1-octyl-3,3-dimethyl-1,3-dihydro-2*H*-indol-2-ylidene)methyl]-3-(dicyanomethylidene)-4-oxocyclobut-1-en-1-olate (2), 5-carboxyl-2,3,3-trimethyl-1-octyl-3*H*-indolium (3), 3-butoxy-4-[(1-octyl-3,3-dimethyl-1,3-dihydro-2*H*-indol-2-ylidene)methyl]-3-cyclobutene-1,2-dione (4), and 2,3,3-trimethyl-1-octyl-3*H*-indolium iodide (6) were synthesized according to reported methods.[14,20]

2-[(1-Octyl-5-carboxy-3,3-dimethyl-1,3-dihydro-2H-indol-2-ylidene)methyl]-3-[cyano(ethoxycarbonyl)methylidene]-4-hydroxycyclobut-1-en-1-olate (5): A solution of 4 (0.93 g, 2.2 mmol), ethyl cyanoacetate (0.28 g, 2.5 mmol), and triethylamine (0.65 mL) in 25 mL of ethanol was stirred for 24 h at reflux temperature. Then the solvent was removed under reduced pressure, and the solid residue was purified by column chromatography on silica gel with 1:20 (v/v) methanol/ethyl acetate to obtain 5 as a red solid (0.5 g, 45% yield). ^{1}H NMR (400 MHz, $CDCl_3$) δ 8.09 (d, J = 8.4 Hz, 1H), 7.97 (s, 1H), 6.90 (d, J = 8.4 Hz, 1H), 5.49 (s, 1H), 4.86 (t, J = 6.8 Hz, 2H), 4.57 (t, J = 7.6 Hz, 2H), 1.87 (m, 2H), 1.64 (s, 6H), 1.52 (m, 2H), 1.38 (m, 4H), 1.27 (m, 6H), 1.01 (t, J = 4.0 Hz, 3H), 0.86 (t, J = 7.2 Hz, 3H).

HSQ2: A mixture of **2** (0.18 g, 0.5 mmol) and **3** (0.2 g, 0.5 mmol) was refluxed in a Dean–Stark apparatus for 24 h in 10 mL of 1:1 (v/v) toluene/*n*-butanol under argon. After removal of the solvent under reduced pressure, the residue was purified by column chromatography on silica gel with 1:10 (v/v) methanol/chloroform to yield HSQ2 as a violet solid (0.29 g, 82% yield).^{1}H NMR (400 MHz, DMSO-d_6) δ: 8.04 (s, 1H), 7.97(d, J = 8.4 Hz, 1H), 7.60 (d, J = 8.4 Hz, 1H), 7.53 (d, J = 8.4 Hz, 1H), 7.43 (t, J = 8.4 Hz, 2H), 7.33 (t, J = 7.8 Hz, 1H), 6.43 (s, 1H), 6.31 (s, 1H), 4.11 (m, 2H), 4.01 (m, 2H), 1.71 (m, 16H), 1.38 (m, 4H), 1.31–1.28 (m, 4H), 1.26–1.20 (m, 12H), 0.83 (t, J = 7.2 Hz, 6H). ^{13}C NMR (100 MHz, DMSO-d_6) δ: 173.72, 172.81, 170.58, 167.49, 166.92, 166.70, 163.56, 145.98, 142.81, 142.08, 141.82, 130.75, 128.80, 126.05, 123.62, 122.88, 118.73, 112.37, 110.77, 89.67, 88.85, 50.12, 48.83, 44.74, 44.14, 31.55, 29.09, 29.05, 28.97, 28.94, 27.42, 27.05, 26.64, 26.26, 26.08, 22.51, 14.4. HRMS (ESI, m/z): calcd for $C_{46}H_{56}N_4O_3$ $[M\text{-}H]^-$: 712.43469; found, 711.42796. Anal. calcd for $C_{46}H_{56}N_4O_3$: C 77.49, H 7.92, N 7.86; found: C 77.03, H 7.92, N 7.64.

HSQ3: A mixture of **5** (0.25 g, 0.5 mmol) and **6** (0.2 g, 0.5 mmol) in 10 mL of 1:1 (v/v) toluene/*n*-butanol was refluxed in a Dean–Stark apparatus for 24 h under argon. After removal of the solvent under reduced pressure, the residue was purified by column chromatography on silica gel with 1:10 (v/v) methanol/chloroform to yield HSQ3 as a violet solid (0.27 g, 72% yield). ^{1}H NMR (400 MHz, DMSO-d6) δ: 7.99 (s, 1H), 7.95 (d, J = 8.0 Hz, 1H), 7.57 (d, J = 7.2 Hz, 1H), 7.61 (s, 1H), 7.46 (t, J = 7.2 Hz, 1H), 7.41 (t, J = 8.0 Hz, 1H), 7.35 (t, J = 8.0 Hz, 1H), 7.28 (t, J = 8.0 Hz, 1H), 6.83 (s, 1H), 4.12 (m, 4H), 4.01 (m, 2H), 1.70 (m, 16H), 1.42 (m, 4H), 1.35–1.25 (m, 6H), 1.22 (m, 13H), 0.82 (m, 6H). ^{13}C NMR (100 MHz, DMSO-d6) δ: 175.06, 173.76, 173.26, 169.74, 169.40, 169.04, 168.87, 168.51, 167.61 166.26, 166.08, 162.23, 146.25, 146.09, 143.07, 142.89, 142.34, 142.11, 141.93, 141.80, 130.76, 128.71, 126.02, 125.77, 125.65, 123.59, 122.86, 121.60, 112.15, 95.39, 89.60, 66.46, 59.64, 49.97, 31.67, 31.21, 29.20, 29.15, 29.07, 27.45, 27.06, 26.88, 26.28, 22.59, 19.26, 15.08, 14.44, 14.16. HRMS (ESI, m/z): calcd

for $C_{48}H_{61}N_3O_5$ [M-H]$^-$:759.46112; found, 758.45385. Anal. calcd for $C_{48}H_{61}N_3O_5$: C 75.86, H 8.09, N 5.53; found: C 75.70, H 8.24, N 5.37.

HSQ4: A mixture of **3** (0.22 g, 0.5 mmol) and **5** (0.25 g, 0.5 mmol) in 10 mL of 1:1 (v/v) toluene/*n*-butanol was refluxed in a Dean–Stark apparatus for 24 h under argon. After removal of the solvent under reduced pressure, the residue was purified by column chromatography on silica gel with 1:5 (v/v) methanol/chloroform to yield HSQ4 as a violet solid (0.22 g, 56% yield). ^{1}H NMR (400 MHz, DMSO-d_6) δ: 8.06 (s, 2H), 7.99 (d, J = 8.0 Hz, 2H), 7.61 (s, 1H), 7.47 (t, J = 8.4 Hz, 2H), 6.82 (s, 1H), 4.11 (m, 6H), 1.73 (m, 16H), 1.40 (m, 6H), 1.25 (br, 17H), 0.83 (m, 6H). ^{13}C NMR (100 MHz, DMSO-d_6) δ: 174.83, 172.31, 171.94, 168.80, 168.38, 167.53, 166.13, 165.08, 145.86, 145.70, 142.81, 142.60, 130.77, 126.94, 123.70, 111.20, 95.64, 89.94, 66.73, 63.46, 49.19, 31.66, 31.19, 29.26, 29.16, 29.07, 27.25, 26.56, 26.28, 22.60, 19.27, 14.45, 14.17. HRMS (ESI, m/z): calcd for $C_{49}H_{61}N_3O_7$ M$^+$: 803.45095; found, 803.45040. Anal. calcd for $C_{49}H_{61}N_3O_7$: C 73.20, H 7.65, N 5.23; found: C 72.90, H 7.72, N 5.10.

Measurement and Characterization: UV–vis–NIR spectra were measured in *N,N*-dimethylformamide (DMF) solution or on a TiO_2 film (thickness = 4 μm) with a UV–vis–NIR spectrophotometer (UV-3600, Shimadzu). ^{1}H NMR (400 MHz) and ^{13}C NMR (100 MHz) spectra were measured with a ECS400 spectrometer (JEOL Resonance). Mass spectra were measured on a Shimadzu Biotech matrix-assisted laser desorption ionization mass spectrometer. Cyclic voltammetry was performed on a CH Instruments 624D potentiostat/galvanostat system with a three-electrode cell consisting of a Ag/$AgNO_3$ reference electrode, a working electrode, and a platinum wire counter electrode. The redox potentials of the dyes were measured in dichloromethane containing 0.1 M tetra-*n*-butylammonium hexafluorophosphate. Electrochemical measurements were performed at a scan rate of 100 mV s^{-1}. The geometry and electronic properties of the dyes were calculated using density functional theory (DFT) with the Gaussian09 program package and the B3LYP/6–31G* basis set.[21]

Cell Fabrication and Characterization: A 16-μm main transparent layer of TiO_2 particles (≈20 nm) and a 5-μm scattering layer of TiO_2 particles (≈400 nm) were screen-printed on a fluorine-doped tin oxide conducting glass substrate. A solution of squaraine dye (2×10^{-4} M) in 1:1 (v/v) acetonitrile/*tert*-butyl alcohol was used to coat the TiO_2 film. The electrodes were immersed in the dye solutions at 25 °C and kept there for 4 h. The dye-coated TiO_2 film was used as the working electrode, and platinum-coated conducting glass was used as the counter electrode. The two electrodes were separated by a Surlyn spacer (50 μm thick), and the cell was sealed by heating the polymer frame. The electrolyte was composed of 0.6 M dimethylpropylimidazolium iodide, 0.05 M I_2, and 0.1 M LiI in acetonitrile. The current–voltage characteristics of the cell were measured using a black metal mask with an aperture area of 0.25 cm^2 under standard AM 1.5G sunlight (100 mW cm^{-2}, WXS-155S-10: Wacom Denso Co. Japan).[22] Monochromatic IPCE spectra were measured with monochromatic incident light of 1×10^{16} photons cm^{-2} under 100 mW cm^{-2} in direct-current mode (CEP-2000BX, Bunko-Keiki). Electrochemical impedance spectra were measured with an impedance analyzer (Solartron Analytical, 1255B) connected to a potentiostat (Solartron Analytical, 1287) under AM 1.5G illumination by means of a solar simulator (WXS-155S-10, Wacom Denso Co. Japan). Electrochemical impedance spectra were recorded over a frequency range of 10^{-2}–10^5 Hz at 298 K.

Supporting Information

Supporting Information is available from the Wiley Online Library or from the author.

Acknowledgements

This work was financially supported by Core Research for Evolutional Science and Technology (CREST) of the Japan Science and Technology Agency. The authors also thank Dr. Keitaro Sodeyama and Dr. Yoshitaka Tateyama for useful discussions.

Received: November 7, 2013
Revised: December 10, 2013
Published online: January 28, 2014

[1] a) B. O'Regan, M. Grätzel, *Nature* **1991**, *353*, 737; b) L. Han, A. Islam, H. Chen, C. Malapaka, B. Chiranjeevi, S. Zhang, X. Yang, M. Yanagida, *Energy Environ. Sci.* **2012**, *5*, 6057.

[2] a) A. Hagfeldt, G. Boschloo, L. Sun, L. Kloo, H. Pettersson, *Chem. Rev.* **2010**, *110*, 6595; b) A. Mishra, M. K. R. Fischer, P. Bäuerle, *Angew. Chem. Int. Ed.* **2009**, *48*, 2474; c) Y. Wu, W. Zhu, *Chem. Soc. Rev.* **2013**, *42*, 2039; d) M. Liang, J. Chen, *Chem. Soc. Rev.* **2013**, *42*, 3453; e) S. Zhang, X. Yang, Y , Numata, L. Han, *Energy Environ. Sci.* **2013**, *6*, 1443; f) T. Kitamura, M. Ikeda, K. Shigaki, T. Inoue, N. A. Anderson, X. Ai, T. Q. Lian, S. Yanagida, *Chem. Mater.* **2004**, *16*, 1806; g) N. Cai, J. Zhang, M. Xu, M. Zhang, P. Wang, *Adv. Funct. Mater.* **2013**, *23*, 3539; h) Y. Numata, A. Islam, H. Chen, L. Han, *Energy Environ. Sci.* **2012**, *5*, 8548; i) J. Zhang, Z. Yao, Y. Cai, L. Yang, M. Xu, R. Li, M. Zhang, X. Dong, P. Wang, *Energy Environ. Sci.* **2013**, *6*, 1604; j) J. Liu, Y. Numata, C. Qin, A. Islam, X. Yang, L. Han, *Chem. Commun.* **2013**, *49*, 7587; k) X. Lu, X. Jia, Z.-S. Wang, G. Zhou, *J. Mater. Chem. A* **2013**, *1*, 9697; l) C. Qin, A. Islam, L. Han, *J. Mater. Chem.* **2012**, *22*, 19236; m) H. Tian, X. Yang, R. Chen, R. Zhang, A. Hagfeldt, L. Sun, *J. Phys. Chem. C* **2008**, *112*, 11023; n) S. Qu, C. Qin, A. Islam, J. Hua, H. Chen, H. Tian, L. Han, *Chem. A Asian J.* **2012**, *7*, 2895; o) Y. Wu, M. Marszalek, S. M. Zakeeruddin, Q. Zhang, H. Tian, M. Grätzel, W. Zhu, *Energy Environ. Sci.* **2012**, *5*, 8261; p) G. Zhou, N. Pschirer, J. C. Schneboom, F. Eickemeyer, M. Baumgarten, K. Müllen, *Chem. Mater.* **2008**, *20*, 1808; q) F. Yang, Md. Akhtaruzzaman, A. Islam, T. Jin, A. El-Shafei, C. Qin, L. Han, K. A. Alamry, S. A. Kosa, M. A. Hussein, A. M. Asiri, Y. Yamamoto, *J. Mater. Chem.* **2012**, *22*, 22550; r) H. Tian, X. Yang, R. Chen, A. Hagfeldt, L. Sun, *Energy Environ. Sci.* **2009**, *2*, 674; s) Y. Hua, B. Jin, H. Wang, X. Zhu, W. Wu, M.-S. Cheung, Z. Lin, W.-Y. Wong, W.-K. Wong, *J. Power Sources* **2013**, *237*, 195; t) J. Mao, N. He, Z. Ning, Q. Zhang, F. Guo, L. Chen, W. Wu, J. Hua, H. Tian, *Angew. Chem. Int. Ed.* **2012**, *51*, 9873; u) Y. Hua, S. Chang, D. Huang, X. Zhou, X. Zhu, J. Zhao, T. Chen, W.-Y. Wong, W.-K. Wong, *Chem. Mater.* **2013**, *25*, 2146; v) Y. Hua, S. Chang, H. Wang, D. Huang, J. Zhao, T. Chen, W.-Y. Wong, W.-K. Wong, X. Zhu, *J. Power Sources* **2013**, *243*, 253.

[3] a) T. Bessho, S. M. Zakeeruddin, C.-Y. Yeh, E. W.-G. Diau, M. Grätzel, *Angew. Chem. Int. Ed.* **2010**, *49*, 6646; b) C. Jiao, N. Zu, K.-W. Huang, P. Wang, J. Wu, *Org. Lett.* **2011**, *13*, 3652; c) L-L. Li, E. W-G. Diau, *Chem. Soc. Rev.* **2013**, *42*, 291; d) A. Yella, H.-W. Lee, H. Tsao, C. Yi, A. K. Chandiran, M. K. Nazeeruddin, E. W.-G. Diau, C.-Y. Yeh, S. M. Zakeeruddin, M. Grätzel, *Science* **2011**, *334*, 629; e) Y. Liu, H. Lin, J. T. Dy, K. Tamaki, J. Nakazaki, D. Nakayama, S. Uchida, T. Kubo, H. Segawa, *Chem. Commun.* **2011**, *47*, 4010; f) C. Y. Lee, C. She, N. C. Jeong, J. T. Hupp, *Chem. Commun.* **2010**, *46*, 6090.

[4] a) M. M. Nicholson, in Phthalocyanines: Properties and Applications, ed. C. C. Leznoff, A. B. P. Lever, VCH Publishers, Inc., New York **1993**, pp. 71; b) H. Imahori, T. Umeyama, S. Ito, *Acc. Chem. Res.* **2009**, *42*, 1809; c) J.-J. Cid, J.-H. Yum, S.-R. Jang, M. K. Nazeeruddin, E. Martinez-Ferrero, E. Palomares, J. Ko, M. M. Grätzel, T. Torres, *Angew. Chem. Int. Ed.* **2007**, *46*, 8358; d) M. Kimura, H. Nomoto, N. Masaki, S. Mori, *Angew. Chem. Int. Ed.* **2012**, *51*, 4371; e) B. Lim, G. Y. Margulis, J.-H. Yum, E. L. Unger, B. E. Hardin, M. Grätzel, M. D. McGehee, A. Sellinger, *Org. Lett.* **2013**, *15*, 784.

[5] a) W. J. Wu, F. L. Guo, J. Li, J. X. He, J. L. Hua, *Synth. Met.* **2010**, *160*, 1008; b) J. Tang, W. J. Wu, J. L. Hua, J. Li, X. Li, H. Tian, *Energy Environ. Sci.* **2009**, *2*, 982.

[6] a) T. Geiger, S. Kuster, J.-H. Yum, S.-J. Moon, M. K. Nazeeruddin, M. Grätzel, F. Nüeesch, *Adv. Funct. Mater.* **2009**, *19*, 2720; b) K. Sayama, S. Tsukagoshi, T. Mori, K. Hara, Y. Ohga, A. Shinpou, Y. Abe, S. Suga, H. Arakawa, *Sol. Energy Mater. Sol. Cells* **2003**, *80*, 47; c) J.-Y. Li, C.-Y. Chen, C.-P. Lee, S.-C. Chen, T.-H. Lin, H.-H. Tsai, K.-C. Ho, C.-G. Wu, *Org. Lett.* **2010**, *12*, 5454; d) L. Beverina, R. Ruffo, C. M. Mari, G. A. Pagani, M. Sassi, F. De Angelis, S. Fantacci, J.-H. Yum, M. Grätzel, M. K. Nazeeruddin, *ChemSusChem* **2009**, *2*, 621; e) J. Warnan, F. Buchet, Y. Pellegrin, E. Blart, F. Odobel, *Org. Lett.* **2011**, *13*, 3944; f) Y. Shi, R. B. M. Hill, J.-H. Yum, A. Dualeh, S. Barlow, S. R. Marder, M. Grätzel, M. K. Nazeeruddin, *Angew. Chem. Int. Ed.* **2011**, *50*, 6619; g) J. H. Delcamp, Y. Shi, J.-H. Yum, T. Sajoto, E. Dell'Orto, S. Barlow, M. K. Nazeeruddin, S. R. Marder, M. Grätzel, *Chem. Eur. J.* **2013**, *19*, 1819.

[7] a) A. Dualeh, J. H. Delcamp, M. K. Nazeeruddin, M. Grätzel, *Appl. Phys. Lett.* **2012**, *100*, 173512; b) P. J. Holliman, M. L. Davies, A. Connell, B. V. Velasco, T. M. Watson, *Chem. Commun.* **2010**, *46*, 7256; c) D. Kuang, P. Walter, F. Nuesch, S. Kim, J. Ko, P. Comte, S. M. Zakeeruddin, M. K. Nazeeruddin, M. Grätzel, *Langmuir* **2007**, *23*, 10906.

[8] a) J.-H. Yum, E. Baranoff, S. Wenger, M. K. Nazeeruddin, M. Grätzel, *Energy Environ. Sci.* **2011**, *4*, 842; b) K. Funabiki, H. Mase, A. Hibino, N. Tanaka, N. Mizuhata,Y. Sakuragi , A. Nakashima, T. Yoshida, Y. Kubota, M. Matsui, *Energy Environ. Sci.* **2011**, *4*, 2186.

[9] a) C. Qin, W.-Y. Wong, L. Han, *Chem. A Asian J.* **2013**, *8*, 1706; b) G. Wei, S. Wang, K. Sun, M. E. Thompson, S. R. Forrest, *Adv. Eng. Mater.* **2011**, *2*, 184; c) G. Chen, H. Sasabe, Z. Wang, X. Wang, Z. Hong, Y. Yang, J. J. Kido, *Adv. Mater.* **2012**, *24*, 2768.

[10] J.-H. Yum, P. Walter, S. Huber, D. Rentsch, T. Geiger, F. Nuësch, F. D , Angelis, M. Grätzel, M. K. Nazeeruddin, *J. Am. Chem. Soc.* **2007**, *129*, 10320.

[11] a) T. Ono, T. Yamaguchi, H. Arakawa, *Sol. Energy Mater. Sol. Cells* **2009**, *93*, 831; b) T. Maeda, Y. Hamamura, K. Miyanaga, N. Shima, S. Yagi, H. Nakazumi, *Org. Lett.* **2011**, *12*, 5994; c) M. Kimura, H. Nomoto, H. Suzuki, T. Ikeuchi, H. Matsuzaki, T. N. Murakami, A. Furube, N. Masaki, M. J. Griffith, S. Mori, *Chem. Eur. J.* **2013**, *19*, 7496.

[12] S. Kuster, F. Sauvage, M. K. Nazeeruddin, M. Grätzel, F. Nüesch, T. Geiger, *Dyes Pigm.* **2010**, *87*, 30.

[13] a) G. M. Shivashimpi, S. S. Pandey, R. Watanabe, N. Fujikawa, Y. Ogomi, Y. Yamaguchi, S. Hayase, *Tetrahedron Lett.* **2012**, *53*, 5437; b) A. Otsuka, K. Funabiki, N. Sugiyama, T. Yoshida, M. Minoura, M. Matsui, *Chem. Lett.* **2006**, 666; c) T. Maeda, S. Mineta, H. Fujiwara, H. Nakao, S. Yagi, H. Nakazumi, *J. Mater. Chem. A* **2013**, *1*, 1303.

[14] C. Qin, Y. Numata, S. Zhang, A. Islam, X. Yang, K. Sodeyama, Y. Tatayama, L. Han, *Adv. Funct. Mater.* **2013**, *23*, 3782.

[15] a) S. Martiniani, A. Y. Anderson, C. Law, B. C. O'Regan, C. Barolo, *Chem. Commun.* **2012**, *48*, 2406; b) B.-G. Kim, K. Chung, J. Kim, *Chem. Eur. J.* **2013**, *19*, 5220; c) T. Daeneke, A. J. Mozer, Y. Uemura, S. Makuta, M. Fekete, Y. Tachibana, N. Koumura, U. Bach, L. Spiccia, *J. Am. Chem. Soc.* **2012**, *134*, 16925.

[16] a) L. P. Hammett, *Physical Organic Chemistry*, McGraw-Hill Book Co., Inc., New York, NY, **1940**, Chaps. III, IV, VII; b) D. Ye, X. Li, L. Yan, W. Zhang, Z. Hu, Y. Liang, J. Fang, W.-Y. Wong, X. Wang, *J. Mater. Chem. A* **2013**, *1*, 7622.

[17] U. Mayerhöffer, B. Fimmel, F. Würthner, *Angew. Chem. Int. Ed.* **2012**, *51*, 164.

[18] A. L. Puyad, G. K. Chaitanya, A. Thomas, M. Paramasivam, K. Bhanuprakash, *J. Phys. Org. Chem.* **2013**, *26*, 37.

[19] C. Qin, A. Islam, L. Han, *Dyes Pigm.* **2012**, *94*, 553.

[20] A. L. Tatarets, I. A. Fedyunyaeva, E. Terpetshnig L. D. Patsenker, *Dyes Pigm.* **2005**, *64*, 125.

[21] M. J. Frisch, G. W. Trucks, H. B. Schlegel, G. E. Scuseria, M. A. Robb, J. R. Cheeseman, G. Scalmani, V. Barone, B. Mennucci, G. A. Petersson, H. Nakatsuji, M. Caricato, X. Li, H. P. Hratchian, A. F. Izmaylov, J. Bloino, G. Zheng, J. L. Sonnenberg, M. Hada, M. Ehara, K. Toyota, R. Fukuda, J. Hasegawa, M. Ishida, T. Nakajima, Y. Honda, O. Kitao, H. Nakai, T. Vreven, J. A. Montgomery, J. E. Peralta, F. Ogliaro, M. Bearpark, J. J. Heyd, E. Brothers, K. N. Kudin, V. N. Staroverov, R. Kobayashi, J. Normand, K. Raghavachari, A. Rendell, J. C. Burant, S. S. Iyengar, J. Tomasi, M. Cossi, N. Rega, N. J. Millam, M. Klene, J. E. Knox, J. B. Cross, V. Bakken, C. Adamo, J. Jaramillo, R. Gomperts, R. E. Stratmann, O. Yazyev, A. J. Austin, R. Cammi, C. Pomelli, J. W. Ochterski, R. L. Martin, K. Morokuma, V. G. Zakrzewski, G. A. Voth, P. Salvador, J. J. Dannenberg, S. Dapprich, A. D. Daniels, O. Farkas, J. B. Foresman, J. V. Ortiz, J. Cioslowski, D. J. Fox, Gaussian, Inc., Wallingford CT, Gaussian 09, A.2 Revision, **2009.**

[22] a) N. Koide, L. Han, *Rev. Sci. Instrum.* **2004**, *75*, 2828; b) N. Koide, Y. Chiba, L. Han, *Jpn. J. Appl. Phys.* **2005**, *44*, 4176; c) Y. Chiba, A. Islam, Y. Watanabe, R. Komiya, N. Koide, L. Han, *Jpn. J. Appl. Phys.* **2006**, *45*, L638; d) C. Qin, W. Peng, K. Zhang, A. Islam, L. Han, *Org. Lett.* **2012**, *10*, 2532; e) X. Yang, M. Yanagida, L. Han, *Energy Environ. Sci.* **2013**, *6*, 54; f) L. Han, N. Koide, Y. Chiba, T. Mitate, *Appl. Phys. Lett.* **2004**, *84*, 2433.